Ultrasound Transducers for Large-Scale Metrology: A Performance Analysis for Their Use by the MScMS

Fiorenzo Franceschini, Domenico Maisano, Luca Mastrogiacomo, and Barbara Pralio

***Abstract*—The Mobile Spatial coordinate Measuring System (MScMS) is a distributed wireless-sensor-network-based system used to perform dimensional measurements of large-scale objects. The system consists of a wireless mobile probe with ultrasonic (US) transceivers, the position of which is determined using a distributed constellation of US transceivers arranged around the measuring area. These US transceivers, which are known as Crickets, transmit US signals to each other and measure their time of flight (TOF) to determine the mutual distances. The MScMS is able to calculate the Cartesian coordinates of the object surface points touched by the wireless mobile probe. This paper aims to experimentally evaluate the performance of the US transducers on each of the MScMS Crickets. The experiments are designed and performed by means of a statistical factorial plan to identify the most important factors affecting the transducers' performance on TOF measurements. Particular attention is given to the error derived by the US signal attenuation and the method of US pulse detection. The results are analyzed in detail and fully interpreted. Finally, some considerations about possible actions to improve the MScMS measuring system are given.**

***Index Terms*—Dimensional measurements, factorial plan, large-scale metrology, signal attenuation, threshold detection, time of flight (TOF), ultrasound transducer.**

I. Introduction

ULTRASONIC (US) sensors are used in many fields. In general, the key features of ultrasound transducers change depending on the propagation medium (solid, liquid, or air). One of the most important applications of US transducers is distance measurement, in which the propagation medium of the acoustic signals is typically air. The common applications associated with distance measurement are presence detection, the identification of objects, the measurement of the shape and orientation of workpieces, collision avoidance, room surveillance, liquid level and flow measurement [1]. The US ranging systems are traditionally low cost compared with other technologies, such as laser range measurement systems. Unfortunately, ultrasound ranging systems exhibit low accuracy, low reliability due to reflection of the transmitted signals, and limited range [2]. The US sensors provide high accuracy only in certain working contexts. Excellent performance can be achieved when measuring, for example, short fixed distances and under controlled environmental conditions (temperature and humidity). The most common technique for distance evaluation is by measuring the time of flight (TOF) of the US signal—either from a transmitter to a receiver or using a single transceiver, which transmits the US signal and receives the corresponding reflected signal. Other factors influencing the performance of US sensors are the type of transducers and the signal detection method used (i.e., thresholding, envelope peak, and phase detection, as discussed in Section III). For this reason, different types of transducers can be employed depending on the specific application. Most of the commercially available air US transducers are ceramic based and operate at 40 kHz. Transducers that operate at higher frequencies, such as at 200 kHz, are more limited and more expensive [3].

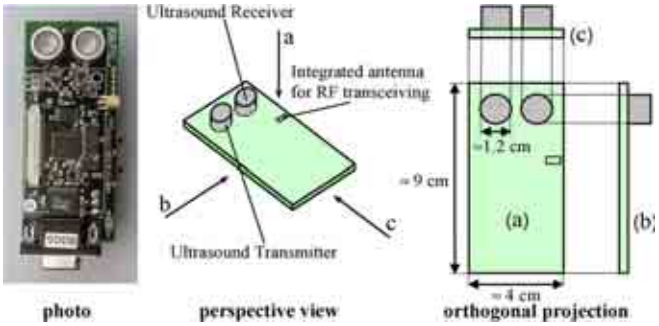

Fig. 1. Cricket device (Crossbow technology) [6].

This paper focuses on the US transducers used by the Mobile Spatial coordinate Measuring System (MScMS). The MScMS is a distributed wireless-sensor-network-based system that is designed to perform dimensional measurements on large-scale objects [4]. In general, the field of large-scale metrology can be defined as the metrology of large machines and structures, specifically "the metrology of objects in which the linear dimensions range from tens to hundreds of meters" [5]. Typical large objects that can be measured using MScMS are airplane wings, fuselages, longerons of railway vehicles, and boat parts.

The MScMS consists of wireless distributed devices—which are known as Crickets—equipped with US transceivers and able to estimate their mutual distances (see Fig. 1) [6]. The first MScMS prototype was developed at the Industrial Metrology and Quality Laboratory, Dipartimento di Sistemi di Produzione ed Economia dell'Azienda, Politecnico di Torino [4].

Manuscript received June 18, 2008; revised April 14, 2009. The Associate Editor coordinating the review process for this paper was Dr. Jennifer Michaels.

The authors are with the Department of Manufacturing Systems and Business Economics (DISPEA), Politecnico di Torino, 10129 Torino, Italy (e-mail: fiorenzo.franceschini@polito.it).

Color versions of one or more of the figures in this paper are available online at http://ieeexplore.ieee.org.

Digital Object Identifier 10.1109/TIM.2009.2022106

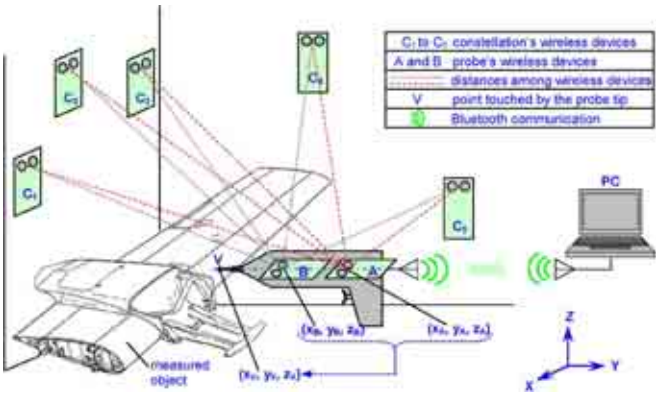

Fig. 2. MScMS representation scheme.

The experimental characterization of the MScMS's US transceiver is performed following an analytical protocol, in which the US signal TOF is identified as the key factor (dependant variable) to be examined. Next, the three independent variables affecting TOF (transmitter–receiver distance, transmitter orientation with respect to the transceiver, and battery charge level of the transmitter) are identified and varied to create a three-way complete block design with repetition within block. Air temperature and humidity are fixed, and the presentation order is completely randomized to minimize the order-of-testing effects. Then, a full factorial analysis of the results is performed using analysis of variance (ANOVA).

This paper is organized into four sections. Section II briefly describes the MScMS structure and features, focusing on the Cricket devices. Section III describes the main features of piezoelectric US transceivers, like those equipping MScMS. Section IV provides a detailed description of the factorial plan, analyzing the effects and the possible interactions of the sources of attenuation. Section V presents and discusses the results of the factorial plan. Finally, the conclusions and future direction of this paper are given.

II. MScMS Description

The MScMS prototype consists of three components (see Fig. 2).

1) A constellation (network) of Cricket devices arranged around the working area.
2) A measuring probe to communicate with the constellation of devices to obtain the coordinates (x, y, z) of the touched points. The measuring probe is a mobile system equipped with a tip to touch the points of the measured objects and a trigger, which is pulled to calculate and store the current coordinates of the probe tip (see Fig. 2). The constellation Crickets act as reference points for locating the measuring probe [7], [8].
3) A computing system to receive and process the data sent by the measuring probe to evaluate the object's geometrical features.

The Cricket devices are developed by the Massachusetts Institute of Technology and produced by Crossbow (see Fig. 1) [6], [9]. Being quite small, light, and potentially cheap, the Cricket devices are compatible with a variety of network configurations [10], [11].

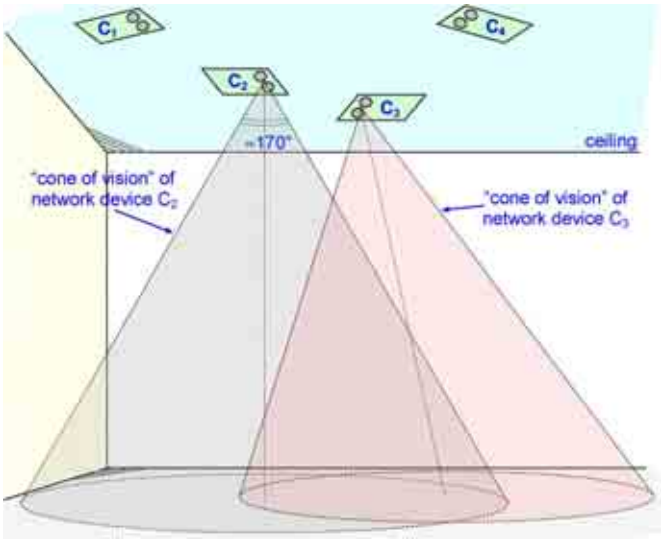

Fig. 3. Representation scheme of the US transmitter "cones of vision."

All the Crickets have RF and US transceivers (see Fig. 1).

They repeatedly communicate and calculate their mutual distances by measuring the TOF of the US signals exchanged [12]. The TOF is multiplied by the speed of sound value to obtain the distance between the two sensors. Due to the RF communication, the Crickets rapidly share the information about their mutual distances. The Crickets, being equipped with an embedded processor and memory, can be programmed by the user and customized depending on the kind of communication to be implemented. This flexibility, as well as their relative low cost, is the main reason for their use in MScMS prototype design.

The measuring probe contains two Cricket devices, which repeatedly determine their distance from the constellation Crickets (see Fig. 2). A Bluetooth transmitter is connected to one of the probe's two Crickets to send this distance information to the PC, which is equipped with an ad hoc software.

While the RF sensor's communication volume is almost omnidirectional and up to 25 m, the US sensors have a communication volume limited by "cones of vision" with an opening angle of about 170° and a range of about 6 m (see Fig. 3). The signal strength inside the cones of vision may be most affected by two factors related to signal attenuation: 1) the distance and 2) the angle from the transmitter's surface. Outside the cones, the signal strength drops to 1% of the maximum value (see the radiation pattern in Fig. 6) [13]. It is critical to take the cone of vision for each US transceiver into account when designing the area of coverage for the constellation of devices. Moreover, to locate the mobile probe's Crickets, they should communicate with at least four constellation devices at once.

Before starting the measurements, the constellation Crickets are placed around the measuring area so that the region of interest is completely covered, with an overlap of at least four devices [14]. Next, they have to be localized, because measurements are possible only if the position of the constellation Crickets is known. To reduce manual operations, a method for a

TABLE I
METROLOGICAL PERFORMANCE OF MScMS IN DETERMINING THE CARTESIAN COORDINATES OF A POINT. MEAN STANDARD DEVIATIONS ARE OBTAINED BY AVERAGING THE STANDARD DEVIATIONS CALCULATED FOR 20 INDIVIDUAL POINTS DISTRIBUTED IN THE WORKING VOLUME

Test	*repeatability*			*reproducibility*		
Mean standard deviation [mm]	σ_x 4.8	σ_y 5.1	σ_z 3.5	σ_x 7.3	σ_y 7.8	σ_z 4.1

semiautomatic localization has been implemented [14]–[17]. It is important to note that reducing the position uncertainty in the localization of constellation nodes is fundamental for reducing the uncertainty in the next mobile probe location.

The measurements consist of three phases.

1) The mobile probe is used to touch the desired points from the part surface.
2) The probe trigger is pulled, and data are sent via Bluetooth to the PC.
3) The Cartesian coordinates (x, y, z) of the points are calculated by the PC.

The PC then uses the Cartesian points to generate a geometrical model of the measured object's surface [15], [17].

The accuracy associated with each TOF measurement generated by each Cricket can be attributed to many factors, such as air turbulence, humidity, air temperature, transducer's relative orientation, and signal bandwidth. The most influential factors are those associated with signal attenuation, which are, respectively, the transmitter–receiver distance, the transmitter orientation with respect to the receiver, and the battery charge level of the transmitter [4], [11].

Today, the MScMS is not very accurate in determining the spatial position of the measured points. This is a consequence of the relatively large uncertainty in TOF measurements. The metrological performance of MScMS was evaluated by two tests: 1) repeatability and 2) reproducibility, which consist of measuring a single point within the working volume and repeating the measurement about 50 times. For the repeatability test, the probe's orientation is kept fixed, whereas for the reproducibility test, the mobile probe orientation is changed measurement by measurement to approach the point from a different direction. Twenty different points in different areas of the working volume are considered for the reproducibility test. For each point, we calculated the standard deviations $(\sigma_x, \sigma_y, \sigma_z)$ associated to the Cartesian coordinates (x, y, z). Table I reports the results obtained from these tests.

In the following, we present a factorial analysis in which the US signal TOF is identified as the dependent variable to be examined, whereas the transmitter–receiver distance, the transmitter orientation with respect to the receiver, and the battery charge level of the transmitter are identified as three possible factors of influence. The results of this analysis can be useful for identifying which factors are most influential on the dependent variable and any possible interactions between them. Generally, factorial analyses—where the different factors vary together—are more efficient than one-factor-at-a-time experiments [18].

III. PIEZOELECTRIC US TRANSDUCERS

In modern US distance measurement systems for industrial applications, piezoelectric transducers clearly dominate. The typical advantages are their compact rugged mechanical design, high efficiency, great range of operation temperature, and relatively low cost. Airborne ultrasound systems have been developed for many types of distance measurement using two possible techniques [19].

1) *Pulse echo*: A transducer emits a burst of ultrasound that bounces off any object in the path of the beam. The transducer then acts as a receiver for the reflected signal. A measurement of the time delay from transmission to reception determines the distance to the target.
2) TOF: A separate transmitter is pointed toward the receiver. Instead of relying on reflections, this system detects the direct transmission of the signal from transmitter to receiver. After measuring the TOF, the sensor's distance can be calculated knowing the speed of sound value.

Cricket devices, being equipped with either a US transmitter and a receiver, implement the TOF technique.

A complex problem when using US transducers is the choice of the characteristic parameters (typically, resonant frequency and bandwidth). For distance measurement with relatively high precision (few millimeters), transducers with a wide bandwidth are needed. The bandwidth is a measure of how rapidly a signal reaches the steady state. A signal at the receiver—which is obtained from transducers with a small bandwidth—slowly climbs from its beginning to its peak in time domain, which causes a relatively large transient time at the receiver. This behavior is shown in Fig. 7 [20], [21].

A second factor affecting the measurement accuracy is the transducer resonant frequency. With increasing frequency (and, thus, reducing wavelength), a better resolution is achievable. Unfortunately, both the transducer bandwidth and the resonant frequency are directly correlated with ultrasound attenuation, and—consequently—they limit the detection range. In other words, considering the same US signal amplitude, the radiated signal amplitude at a given distance from the transmitter becomes smaller if its bandwidth and resonant frequency increase [21], [22]. For this reason, the selection of US frequency and bandwidth is a compromise between accuracy and detection range.

The piezoelectric transducer adopted by Cricket devices is a low-cost general-purpose model [Murata MA40S4R, see Fig. 4(a)] with a relative wide bandwidth [see Fig. 4(b)], in which the center frequency is about 40 kHz. This working frequency is a tradeoff between accuracy (considering the single distances, it is around 1–2 cm) and detection range (up to 6–8 m) [11], [23].

The acoustic strength of the radiation from a flat transducer with "piston motion" (like the Crickets' US transducers) is generally angle dependent because of the phase difference of waves from each point on the surface [19]. The acoustic radiation is the integral sum of the waves from all points on the transmitter surface, and the propagation path difference from each point to a reference observation point has a phase cancellation effect that leads to signal attenuation [24], [25].

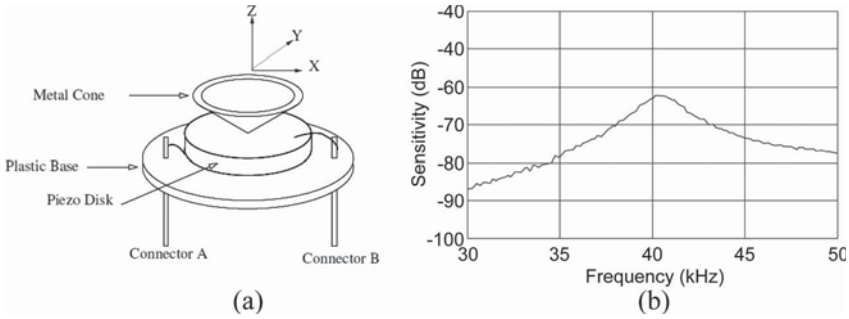

Fig. 4. (a) Internal construction of a Murata MA40S4R piezoelectric US transmitter/receiver. The dimensions of the piezomaterial cause the disk to resonate at a precise frequency (around 40 kHz). (b) Representation of the transmitter bandwidth by means of a frequency response plot.

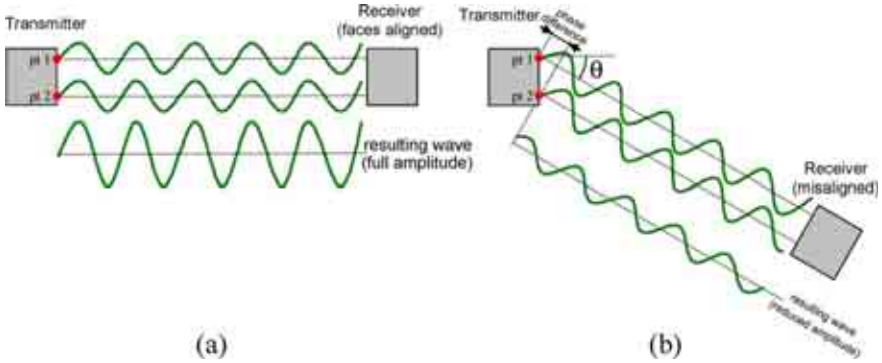

Fig. 5. US signal strength dependence on the transmitter angle (θ). The simplified illustration represents the interaction of the waves from two points on the transducer surface. The resulting wave is given by the sum of the single waves. If the receiver is directly facing the transmitter (case-a), then the two individual waves are in phase, and the resulting wave amplitude has the maximum value. If the transmitter is misaligned with the receiver (case-b), then the resulting wave is attenuated because of a phase-canceling effect due to the phase difference between the two individual waves [24].

However, if the receiver is directly facing the transmitter at sufficient distance from it, the acoustic radiation from each point of the transducer surface does not have a phase-canceling effect. This is because the distance from an arbitrary point on the transducer surface to the receiver becomes almost constant, and the difference is much smaller than the wavelength [26]. On the other hand, if the transmitter is misaligned with the receiver, then the US signal amplitude will be attenuated because of the disruptive interference of the different US signals from different surface points on the transmitter. This effect is represented by the simplified illustration in Fig. 5. The scheme considers the interaction of waves from two points on the transducer surface; the same principle can be extended to all the surface points.

An example of the resulting US transmitter radiation pattern as a function of the transmitter angle with respect to the receiver (misalignment angle) is shown in Fig. 6. As represented, the transmitter US signal strength drops along directions that are away from the direction facing the US transducer.

Similarly, the received signal strength can be influenced by the receiver orientation. Particularly, assuming the same signal strength from the transmitter, the received signal strength is maximum when the receiver's surface is facing the transmitter. On the other hand, the received signal decreases when the receiver's surface is angled.

Several methods have been developed for detecting US signals. Thresholding is the simplest and the most widely used and applies to any type of short-duration signal. In this method, which is used in Crickets, the receiver electric output signal is compared with a threshold level (65 mV for the Crickets)

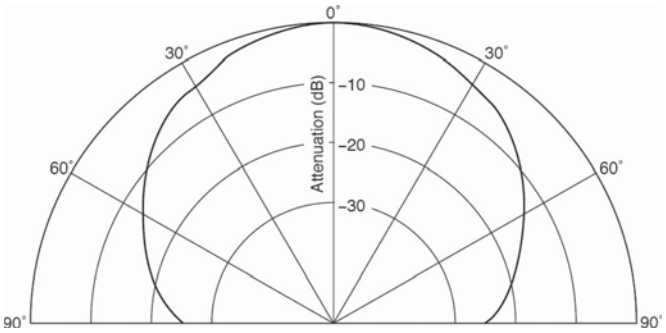

Fig. 6. Radiation pattern of the Cricket US transducer as a function of the orientation on a plane along the transducer's axis. The signal strength drops along the direction that is away from the normal direction to the transducer surface.

such that the arrival of the wave is acknowledged when the signal reaches this level (see Fig. 7). This method depends on the amplitude of the pulse received: the larger the signal amplitude, the smaller the time taken by the signal before reaching the threshold. For example, in Fig. 7, when the signal has a full amplitude, the detection threshold is first exceeded by the second peak of the ultrasound waveform. When the waveform is attenuated by a factor of 0.50 (half amplitude signal), the detection threshold is first exceeded by the third peak of the ultrasound waveform. If the channel attenuation is quite significant, then it may cause the threshold to be exceeded a few periods late instead of just one period late. Considering that at 40 kHz the period is 25 μs, the error will be approximately in integer multiples of 25 μs. The error in the TOF evaluation

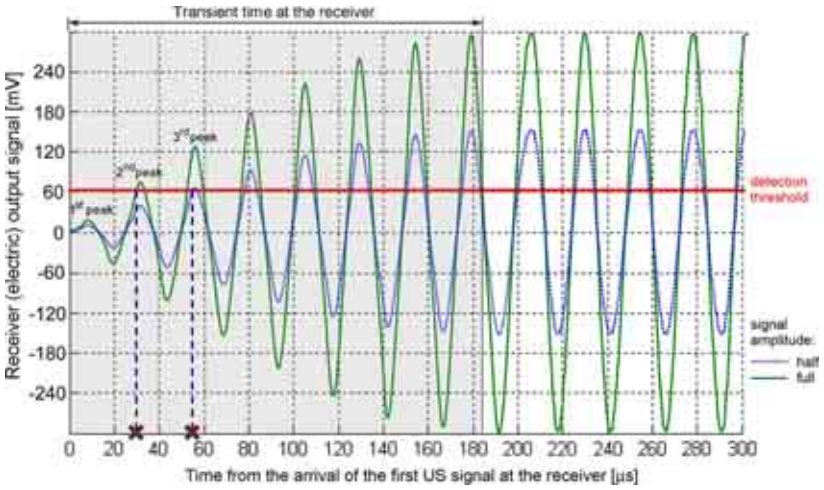

Fig. 7. Graphical representation of thresholding detection. A minimum number of cycles are necessary to bring the receiver to steady-state conditions (transient time at the receiver) [31]. The error in the distance measurement is dependent upon the received US signal amplitude. The time taken for the received signal to reach the threshold is dependent on its amplitude.

results in an error in the distance estimation. The speed of sound is about 340 m/s, so one ultrasound time period corresponds to a distance of about $25 \cdot 340/1000 = 8.5$ mm. In practice, the threshold can be exceeded by up to four periods late, so the distance overestimation can be up to 3–4 cm!

A modification of thresholding is "envelope peak detection," which may be called adjustable thresholding. This method acknowledges the arrival of the signal when a maximum amplitude is detected; therefore, it does not depend upon the absolute magnitude of the pulse, only upon its shape. As a consequence, it is more accurate and robust than simple magnitude thresholding, where the acknowledge time can easily jump by one period.

Other more refined ranging methods are based on phase detection with fixed-frequency signals and with frequency-modulated signals. These methods, however, require complex hardware and software. They use a digital signal processor to process the phase measurements to overcome the inherent range limitation of one wavelength [2], [27]–[29].

Recently, a lot of effort has been done to incorporate pulse compression techniques to the US sensory system to improve the accuracy in distance measurements using relatively simple hardware and software [30].

IV. Factors Affecting US Transceivers

The MScMS measurement accuracy may change depending on many different factors related to the use of US transceivers, such as temperature, humidity, air turbulence, transducer geometry, transducer bandwidth, and US signal attenuation. When implementing a thresholding detection method, the TOF measurement errors are mostly due to the factors related to US signal attenuation. The typical sources of attenuation are the following [4], [6]:

1) distance between transceivers;
2) angle of one transmitter with respect to the transceiver (misalignment angle);
3) transducer battery charge level.

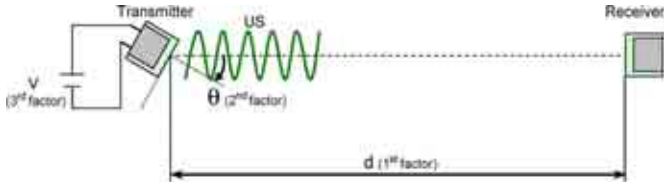

Fig. 8. US sensor experimental setup.

With the aim of investigating the effect of these factors on TOF measurements, a complete experimental factorial plan is built.

Fig. 8 shows an illustration of the following experimental setup.

1) The transmitter and receiver are positioned facing each other.
2) The distance (d—first factor) between transceivers is known.
3) The transmitter face is not perfectly aligned with the receiver face. A misalignment angle (θ—second factor) with regard to the transmitter face is introduced. The receiver face is kept perpendicular to the ultrasound wave direction of propagation.
4) The transmitter battery charge level is monitored by measuring the battery potential difference (V—third factor). Each Cricket is equipped with two AA rechargeable 2700-mAh batteries connected in series. Their potential difference is measured by a standard voltmeter. The potential difference is not a direct measurement of the battery charge level, but—since they are correlated—it is a useful indicator of it.

The TOF is measured by changing these three factors at different levels.

1) Seven levels for θ (transmitter rotations from 0° to 60° in 10° intervals). For larger angles, the transmitter and receivers do not easily communicate because of the rapid decrease in the US signal for angles greater than 60° (see Fig. 6).

TABLE II
LIST OF THE EXPERIMENTS CARRIED OUT ON THE CRICKET'S US TRANSDUCERS

	Factors		
	1st – Transceivers distance (d)	2nd – Transmitter misalignment angle (θ)	3rd – Battery level (V)
Levels	(Short) $d_1 = 1160$ mm	$\theta_1 = 0°$	
		$\theta_2 = 10°$	$V_1 = 2.7$ V
	(Medium) $d_2 = 2034$ mm	$\theta_3 = 20°$	$V_2 = 2.6$ V
		$\theta_4 = 30°$	$V_3 = 2.5$ V
		$\theta_5 = 40°$	$V_4 = 2.4$ V
	(Long) $d_3 = 3671$ mm	$\theta_6 = 50°$	$V_5 = 2.3$ V
		$\theta_7 = 60°$	

- all the possible $7 \cdot 3 \cdot 5 = 105$ different combinations are carried out in random order;
- for each combination, TOF measurements are repeated 50 times and the average value is taken;
- all the 105 combinations above are replicated 5 times; consequently, the total number of combinations is 525.

2) Three levels for d: short, medium, and long distance between transceivers. These distances have been measured using three reference bars, which were accurately calibrated using a standard coordinate measuring machine (uncertainty with a standard deviation of less than a hundredth of millimeters) [32].
3) Five levels for V (from 2.3 to 2.7 V in 0.1-V intervals).

Table II provides a summary of the combinations for the three factor levels.

There are $7 \cdot 3 \cdot 5 = 105$ different combinations to be carried out. The test sequence is randomized using the random number generator provided by Minitab. For each of these combinations, 50 measurements of the TOF are performed, taking the average value. All the measurements have been replicated five times. The total number of combinations analyzed is $105 \cdot 5 = 525$.

The response variable considered in the factorial plan is the TOF error, which is defined as follows:

$$\text{TOF-Error} = (\text{Measured-TOF} - \text{Expected-TOF}) \quad (1)$$

where

Measured-TOF — TOF measured by a pair of Crickets;

Expected-TOF $= (d/s)$ — where (d) is the transceiver's known distance, and (s) is the speed of sound in the experimental conditions. For example, with a temperature $T = 24$ °C and a relative humidity RH $= 27\%$, (s) is about 346 m/s.

TOF-Error is used as an indicator of the error in TOF evaluation.

The experiments are performed in a controlled environment ($T = 24$ °C and RH $= 27\%$).

V. ANALYSIS OF THE EXPERIMENTAL RESULTS

Section V-A shows and discusses the results of the factorial plan. Section V-B summarizes them, providing theoretical interpretations of some of the important aspects. Section V-C presents other minor experiments, which are aimed at deepening the factorial plan analysis.

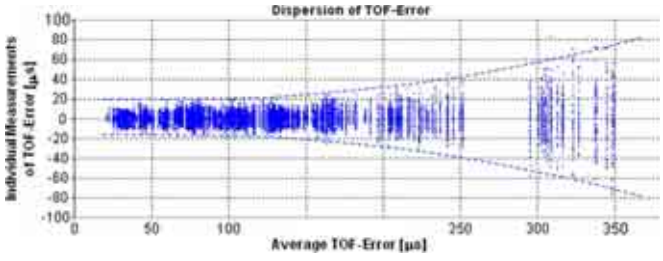

Fig. 9. TOF-Error standard deviation versus average TOF-Error. For each of the 525 factor combinations, the variables are calculated using the corresponding 50 repeated TOF-Error measurements.

A. Results of the Factorial Plan

Analyzing the factorial plan experimental outputs, the first interesting result is that the TOF-Error standard deviation (σ) changes depending on the TOF-Error value. This behavior is illustrated in Fig. 9, where for each of the 525 factorial plan combinations the average TOF-Error and the respective standard deviation—which are calculated using the corresponding 50 repeated measurements—are plotted. It can be noticed that the larger the average TOF-Error value, the larger the individual measurement dispersion. The nonhomogeneity of the TOF-Error variance is also tested through Levene's statistical test at $p < 0.05$.

Since the assumption of homogeneity of the TOF-Error variances is violated, ANOVA cannot properly be applied to verify whether factors have a significant effect on the response (TOF-Error) and whether there are factor interactions [18]. The usual approach to dealing with nonhomogeneous variance is to apply a *variance-stabilizing transformation*. In this approach, the conclusions of the ANOVA will apply to the transformed populations. The most common transformation is the exponential $y^* = y^\lambda$, where λ is the parameter of the transformation. Box and Cox proposed an optimization method for determining the transformation parameter [33].

Once a value of λ is selected by the Box–Cox method, the experimenter can analyze the data using y^* as the transformed response (it will be identified hereafter as "corrected TOF-Error"). In our specific case, the obtained transformation parameter is $\lambda = 0.52$. Applying Levene's test to the transformed response, the resulting variance no longer violates the test's null hypothesis of homogeneity.

Of course, a problem is that it may be unpractical working with the transformed response (y^*) in the transformed scale, since it can result in a nonsensical value over the factor space of interest. To construct a model in terms of the original response, the opposite change of variable—$(y^*)^{1/\lambda}$—is performed.

The Main Effects Plot represents the single examined factors effect on the TOF-Error (see Fig. 10). The points in the plot are the means of the response variable at the various levels of each factor (for each level of the examined factor, the mean is calculated by averaging all the responses obtained and changing the remaining two factors). A reference line is drawn at the grand mean of the response data. This kind of plot is useful for comparing the magnitudes of the main effects.

The qualitative result is that the misalignment angle and the transmitter–receiver distance have an important effect, whereas the effect of the battery charge level is minor.

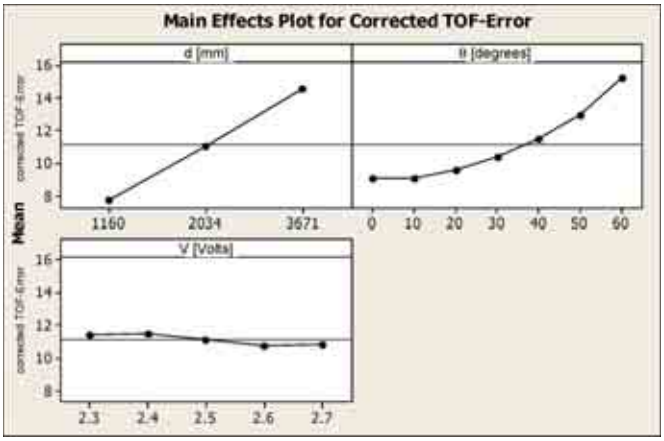

Fig. 10. Main effect plot for means related to the three examined factors: θ (misalignment angle), d (transmitter–receiver distance), and V (batteries potential difference).

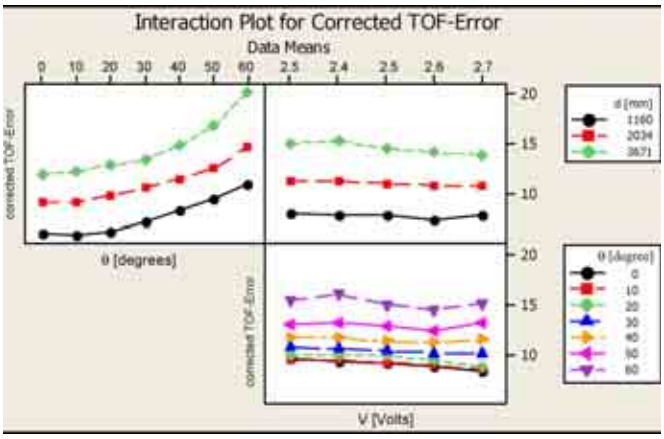

Fig. 11. Interaction plot for the corrected TOF-Error considering the three factors (d, θ, and V).

To qualitatively judging the presence of interactions among the three factors, an Interaction Plot is constructed in Fig. 11. This plot represents the means for each level of a factor with the level of a second factor held constant (considering two factors, for each combination of their levels, the mean is calculated by averaging the responses obtained by changing the remaining factor). The interaction between two levels is present when the response at a factor level depends upon the level(s) of the other factors. Parallel lines in an interaction plot indicate no interaction. The greater the departure of the lines from the parallel state, the higher the degree of interaction [18].

Fig. 11 shows that the two-way interactions are negligible, and that the main effects presented in Fig. 10 are consistent within each factor level.

The results of the factorial plan are examined by ANOVA (see Fig. 12). ANOVA is best suited to data sets in which the independent variables are discrete; for this reason, the levels of d, θ, and V are "discretized."

In ANOVA, the variance related to the response is partitioned into contributions due to the different factors and their interactions. The results of ANOVA can be considered reliable as long as the following assumptions are met: 1) The response variable is normally distributed; 2) The data are independent; and 3) The

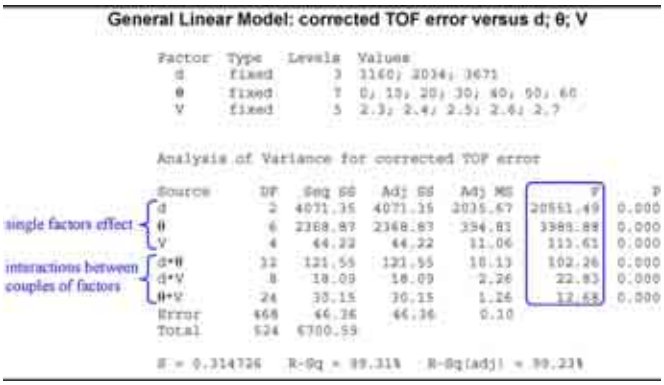

Fig. 12. ANOVA applied to the (transformed) response of the factorial plan.

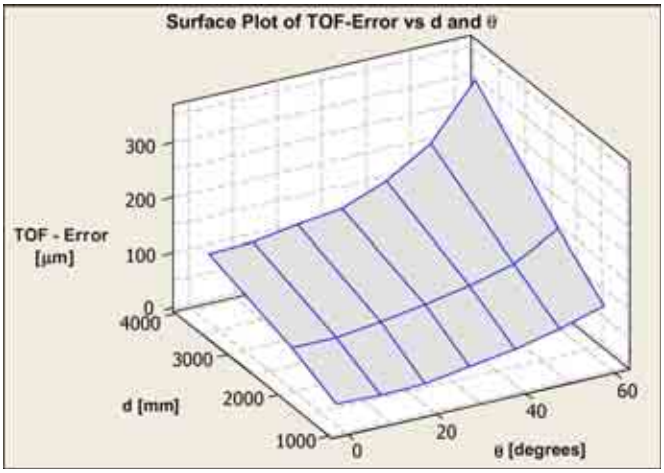

Fig. 13. Surface plot to represent the effect of the interaction of factors d and θ on the TOF-Error.

variances of the populations are equal. After applying the Box–Cox response transformation, all these assumptions are satisfied. In particular, the assumption of normal distribution is verified by the Anderson–Darling normality test at $p < 0.05$.

Analyzing the ANOVA results, all three factors and their two-way interactions are found to be significant based on Fisher's test at $p < 0.05$. With regard to the effect of the single factors, the most important are d and θ, whereas the effect of V is minor (a small F value). This is consistent with the Main Effects Plot in Fig. 10. With regard to the factor interactions, they are all statistically significant (p values lower than 0.05) but very weak. The strongest is the interaction between d and θ. The effect of this interaction on the TOF-Error is represented by the surface plot in Fig. 13. As shown, the composition of large misalignment angles (θ) and large distances (d) produces TOF-Errors that are larger than those obtained by adding the effects of the single factors, taken separately.

Another representation of the experimental outputs is given in Fig. 14, where the average TOF-Error and the corresponding standard deviation (calculated for each combination of factors using the 50 repeated measurements) are plotted depending on V and θ for each of the three transmitter–receiver distances.

As already indicated, the TOF-Error increases with an increase in θ and d. In addition, the TOF standard deviation slightly increases with an increase in angle; this behavior is

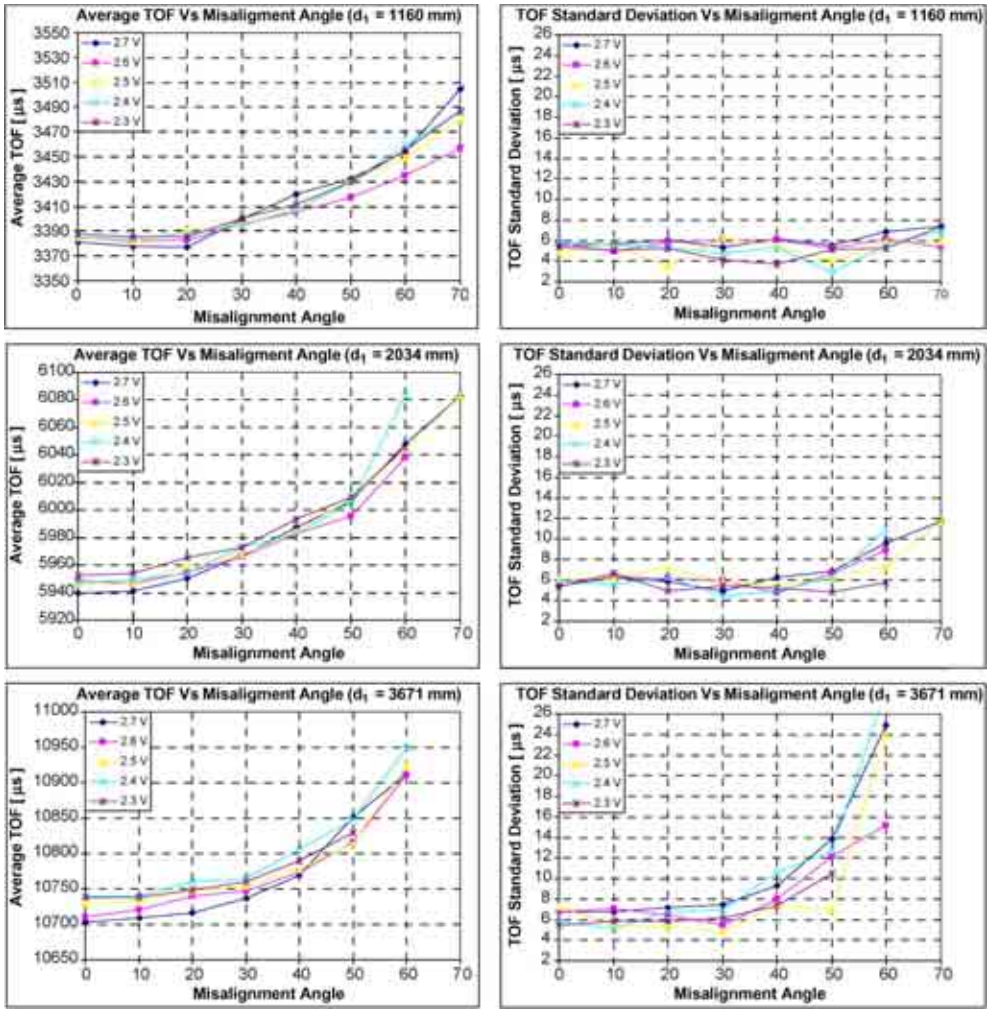

Fig. 14. TOF average value and standard deviation depending on the misalignment angle (θ) and the battery level (V) for different transmitter–receiver distances.

more pronounced for large distances between transmitter and receiver.

Fig. 14 includes other measurements not included in the factorial plan: the TOF-Error measurements related to misalignment angles of 70°, which cannot be performed for all the distances between transceivers (d_1, d_2, and d_3). For instance, considering the long distance ($d_3 = 3871$ mm), the transmitter and receiver are not able to communicate because of the strong signal attenuation. Finally, these graphs show that the effect of factors θ and d on the TOF-Error is evident, whereas the effect of the battery charge level (V) is small.

TOF-Error is always positive because of the TOF overestimation due to signal attenuation (which is proportional to d, θ, and V). The effect of the transmitter–receiver distance on the TOF-Error is also shown in Fig. 15, plotting the TOF-Error versus the transmitter–receiver distance for different misalignment angles.

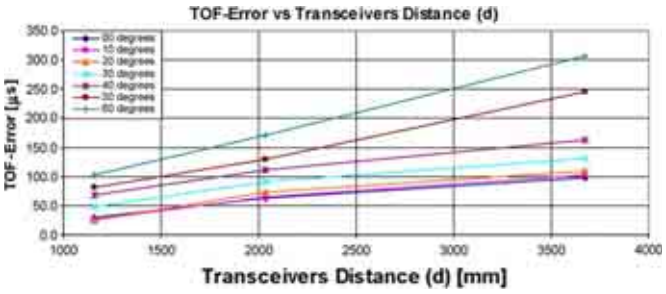

Fig. 15. TOF-Error depending on the transmitter–receiver distance (d). The plotted curves are related to the different transmitter misalignment angles (θ). The effect of the signal attenuation (TOF overestimation) increases with the transceiver distance.

B. Interpretation of the Results

In summary, the TOF-Error is influenced by three factors related to the US signal attenuation.

1) The most important are the transducer distance (d) and the misalignment angle (θ).
2) The effect of the transceiver battery charge level (V) is minor.
3) The most significant two-way interaction is between factors d and θ.

The TOF-Error standard deviation changes depending on the received US signal attenuation. Here follows an explanation of this behavior. The amplitude of the US signals at the transmitter is not perfectly stable, but rather has a certain natural variability derived by many sources, such as power and

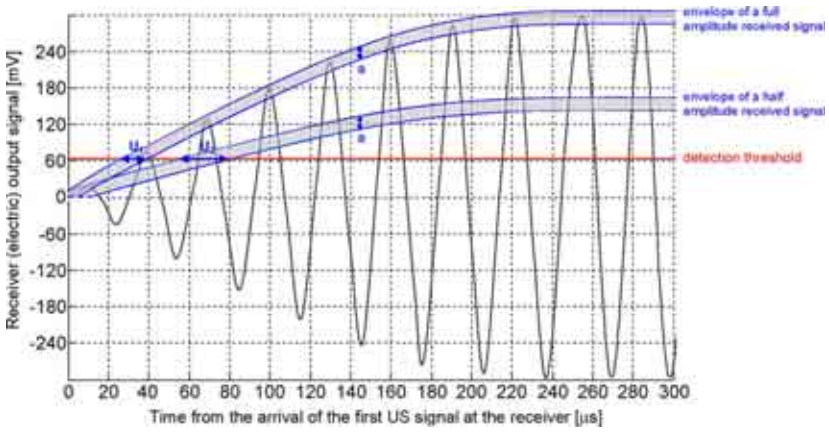

Fig. 16. Considering the same variability (ΔV) in the receiver voltage signal and the corresponding uncertainty in the TOF changes. The more attenuated the signal, the larger the TOF variability.

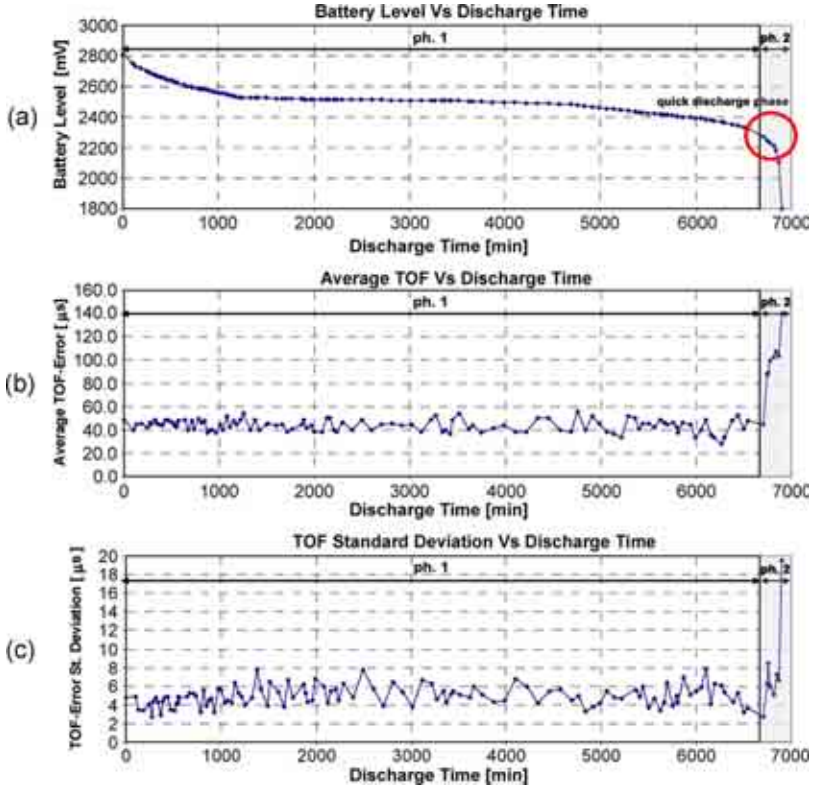

Fig. 17. (a) Battery level, (b) average TOF-Error, and (c) TOF-Error standard deviation depending on the Cricket device battery discharge time. Each point value is calculated over 100 individual measurements.

control supply, air temperature, air turbulence, and signal bandwidth. The envelope of the US signal amplitude at the receiver is included within an uncertainty band (highlighted in grey in Fig. 16).

Considering signals with different amplitudes and assuming the uncertainty bandwidth to be the same, the larger the transient slope, the lower the TOF-Error uncertainty ("U_1" and "U_2" in Fig. 16).

Of course, the behavior previously described is a consequence of the use of the thresholding detection method at the US receivers. The Cricket's accuracy could be improved by implementing a more refined ultrasound detection method that is able to exactly calculate the precise instant in which the US signal is received [30].

C. Additional Experiments

The two following paragraphs present two additional experiments, which are aimed at deepening the analysis carried out by the factorial plan. They are the following:

1) complete battery discharge cycle to investigate in detail the relationship between the battery level and the error in the TOF evaluation;
2) analysis of the repeatability of Cricket devices in the TOF measurements.

D. Analysis of the Cricket Device Battery Discharge

According to the results of the factorial plan, the battery charge level has a small effect on TOF-Error. However,

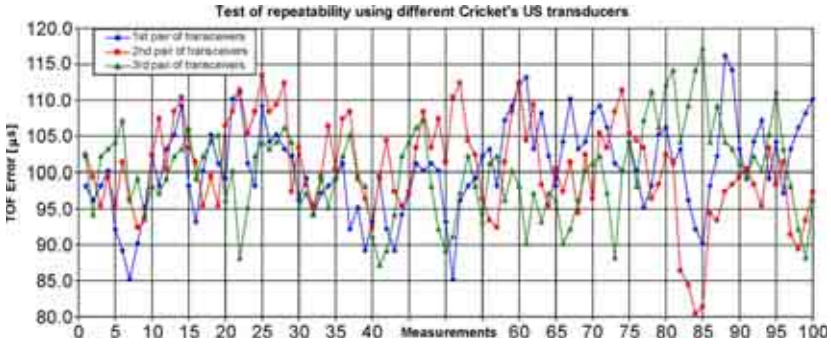

Fig. 18. Plot of TOF-Error from different Cricket's US transducers.

One-way ANOVA: TOF-Error vs pairs of Cricket transceivers

Source	DF	SS	MS	F	P
factor	2	26.6	13.3	0.33	0.720
Error	297	12019.9	40.5		
Total	299	12046.6			

S = 6.362 R-Sq = 0.22% R-Sq(adj) = 0.00%

Individual 95% CIs For Mean Based on Pooled StDev

Level	N	Mean	StDev
1	100	100.72	6.26
2	100	100.04	6.15
3	100	100.61	6.67

overlapping region

99.20 100.00 100.80 101.60

Pooled StDev = 6.36

Tukey 95% Simultaneous Confidence Intervals

All Pairwise Comparisons between different pairs of Cricket transceivers

Individual confidence level = 98.01%

factor = 1st pair subtracted from:

factor	Lower	Center	Upper
2nd pair	-2.786	-0.680	1.426
3rd pair	-2.216	-0.110	1.996

-1.5 0.0 1.5 3.0

factor = 2nd pair subtracted from:

factor	Lower	Center	Upper
3rd pair	-1.536	0.570	2.676

-1.5 0.0 1.5 3.0

Fig. 19. Results of ANOVA and Tuckey's test to examine the Cricket's US transducer's repeatability.

abnormal TOF-Error measurements were noticed during the last part of the Cricket device's battery life. This test aims at studying the relationship between the battery charge level and the error in the TOF evaluation. It consists of measuring TOF-Error at more than a hundred different transmitter battery levels, from a full charge to a complete battery discharge.

The Transmitter and receiver are positioned at the known distance of 1582 mm, with their faces perfectly aligned ($\theta = 0°$).

The results are reported in Fig. 17. Two characteristic phases can be identified in the curves plotted in Fig. 17.

1) The battery charge level very slowly decreases with the battery life time. The average TOF-Error and the TOF-Error standard deviation are not significantly influenced by the battery level.
2) In the final part of the battery life (potential difference lower than 2.3 V), the discharge is very quick, and the measured potential difference rapidly falls to zero. This phase is characterized by a "knee" in the battery charge level curve. In this phase, the corresponding TOF-Error average value and the standard deviation "explode."

As a result, to avoid an incorrect estimate of TOF, it is important to replace the batteries before they reach the "quick discharge phase." To reach this purpose, it can be helpful to control the Cricket battery level through a firmware utility [34].

E. Test of Repeatability of the US Transducers

The US transceiver's repeatability is tested by positioning three different pairs of Cricket transceivers at the same distance (3633 mm) with their faces perfectly aligned. For each pair of devices, 100 different individual TOF-Error measurements are acquired.

The data are analyzed by a one-factor ANOVA to test the null hypothesis that there is no difference in the TOF-Error mean values measured by different couples of transceivers (the examined factor). As expected, the TOF-Error does not significantly change depending on the different Cricket devices used. Fig. 18 shows the plot of the TOF-Error measured 100 times under the same conditions using three different pairs

of Cricket transceivers. As shown, the measurements obtained using different devices generally overlap.

Consequently, it can be said that the use of different US transducer devices does not influence the TOF-Error. This qualitative impression is confirmed by the results of ANOVA and Tuckey's comparison test, as shown in Fig. 19.

VI. Conclusion

This paper has analyzed the most important sources of error related to the TOF measurements performed by the US transducers with which MScMS is equipped. The measurement error may change depending on many different factors; however, the most important effects are due to the US signal attenuation, which may have three major sources: 1) transmitter–receiver distance; 2) transceiver misalignment angle; and 3) transducer battery level. In particular, this paper shows that the transducer misalignment and the transmitter–receiver distance are the most influential factors. This statement is supported by the results of an experimental factorial plan. It is important to remark that this source of error is directly caused by the thresholding detection method of ultrasound. In addition, these results can be useful to identify the major MScMS sources of inaccuracy and to determine how the error in TOF evaluation changes in the different points within the Cricket transmitters' "cones of vision." An organic analysis of the combined effect of the transmitter and receiver orientations on TOF-error will be the object of a future work.

Regarding the future, the Cricket's accuracy could be improved by using more refined ranging methods based on US pulse compression. This should be obtained with not very complex modifications to the current Cricket hardware and firmware. Another possible solution to the error associated with transmitter misalignment is the use of US transducers, which presents a smaller directivity, such as cylindrical polyvinylidene fluoride film transducers [3], [26], [27]. The TOF measurement error can also be reduced by implementing proper compensation and/or correction techniques based on the results of the analysis presented in this paper.

References

[1] C. Delepaut, L. Vandendrope, and C. Eugène, "Ultrasonic three-dimensional detection of obstacles for mobile robots," in *Proc. 16th ISIR*, Brussels, Belgium, 1986, pp. 483–490.

[2] W. Manthey, N. Kroemer, and V. Magori, "Ultrasonic transducers and transducer arrays for applications in air," *Meas. Sci. Technol.*, vol. 3, no. 3, pp. 249–261, Mar. 1992.

[3] M. Toda, "Cylindrical PVDF film transmitters and receivers for air ultrasound," *IEEE Trans. Ultrason., Ferroelectr., Freq. Control*, vol. 49, no. 5, pp. 626–634, May 2002.

[4] F. Franceschini, M. Galetto, D. Maisano, and L. Mastrogiacomo, "Mobile Spatial coordinate Measuring System (MScMS)—Introduction to the system," *Int. J. Prod. Res.*, vol. 47, no. 14, pp. 3867–3889, 2009. DOI: 10.1080/00207540701881852.

[5] M. J. Puttock, "Large-scale metrology," *Ann. CIRP*, vol. 21, no. 1, pp. 351–356, 1978.

[6] *Cricket v2 User Manual*, MIT Comput. Sci. Artif. Intell. Lab, Cambridge, MA, 2004. [Online]. Available: http://cricket.csail.mit.edu/v2man.html

[7] N. Patwari, J. Ash, S. Kyperountas, A. Hero, III, R. Moses, and N. Correal, "Locating the nodes—Cooperative localization in wireless sensor networks," *IEEE Signal Process. Mag.*, vol. 22, no. 4, pp. 54–69, Jul. 2005.

[8] J. M. Martin, A. R. Jiménez, F. Seco, L. Calderon, J. L. Pons, and R. Ceres, "Estimating the 3D-position from time delay data of US-waves: Experimental analysis and new processing algorithm," *Sens. Actuators A, Phys.*, vol. 101, no. 3, pp. 311–321, Oct. 2002.

[9] *Crossbow Technology*, 2008. [Online]. Available: http://www.xbow.com

[10] N. B. Priyantha, A. Chakraborty, and H. Balakrishnan, "The cricket location-support system," in *Proc. 6th ACM MOBICOM*, Boston, MA, Aug. 2000, pp. 32–43.

[11] H. Balakrishnan, R. Baliga, D. Curtis, M. Goraczko, A. Miu, N. B. Priyantha, A. Smith, K. Steele, S. Teller, and K. Wang, "Lessons from developing and deploying the cricket indoor location system," MIT, Tech. Rep., 2003.

[12] F. Gustafsson and F. Gunnarsson, "Positioning using time difference of arrival measurements," in *Proc. IEEE ICASSP*, Hong Kong, 2003, vol. 6, pp. 553–556.

[13] N. B. Priyantha, H. Balakrishnan, H. D. Demaine, and S. Teller, "Mobile-assisted localization in wireless sensor networks," in *Proc. 24th Annu. Joint Conf. IEEE Commun. Soc. Comput. Commun. (INFOCOM)*, Miami, FL, Mar. 13–17, 2005, vol. 1, pp. 172–183.

[14] F. Franceschini, M. Galetto, D. Maisano, and L. Mastrogiacomo, "The problem of distributed wireless sensors positioning in the Mobile Spatial coordinate Measuring System (MScMS)," in *Proc. 9th Biennial ASME Conf. ESDA*, Haifa, Israel, Jul. 7–9, 2008.

[15] F. Franceschini, M. Galetto, D. Maisano, and L. Mastrogiacomo, "A review of localization algorithms for distributed wireless sensor networks in manufacturing," *Int. J. Comput. Integr. Manuf.*, vol. 22, no. 7, pp. 698–716, 2009. DOI: 10.1080/09511920601182217 2008.

[16] A. Mahajan and F. Figueroa, "An automatic self-installation and calibration method for a 3D position sensing system using ultrasonics," *Robot. Auton. Syst.*, vol. 28, no. 4, pp. 281–294, Sep. 1999.

[17] D. Moore, J. Leonard, D. Rus, and S. S. Teller, "Robust distributed network localization with noisy range measurements," in *Proc. SenSys*, Baltimore, MD, 2004, pp. 50–61.

[18] D. C. Montgomery, *Design and Analysis of Experiments*, 7th ed. New York: Wiley, 2008.

[19] A. C. Berners, J. G. Webster, C. J. Worringham, and G. E. Stelmach, "An ultrasonic time-of-flight system for hand movement measurement," *Physiol. Meas.*, vol. 16, no. 4, pp. 203–211, Nov. 1995.

[20] B. Cheng and T. Chang, "Enhancing ultrasonic imaging with low transient pulse shaping," *IEEE Trans. Ultrason., Ferroelectr., Freq. Control*, vol. 54, no. 3, pp. 627–635, Mar. 2007.

[21] C. C. Tong, J. F. Figueroa, and E. Barbieri, "A method for short or long range time-of-flight measurements using phase-detection with an analog circuit," *IEEE Trans. Instrum. Meas.*, vol. 50, no. 5, pp. 1324–1328, Oct. 2001.

[22] R. Kažys, L. Mažeika, R. Šliteris, and A. Voleišis, "Online profiling of nonplanar objects by high-resolution air-coupled ultrasonic distance measurements," *IEEE Trans. Instrum. Meas.*, vol. 56, no. 5, pp. 1825–1830, Oct. 2007.

[23] V. Magori and H. Walker, "Ultrasonic presence sensors with wide range and high local resolution," *IEEE Trans. Ultrason., Ferroelectr., Freq. Control*, vol. UFFC-34, no. 2, pp. 202–211, Mar. 1987.

[24] J. Lamancusa and J. F. Figueroa, "Ranging errors caused by angular misalignment between ultrasonic transducer pairs," *J. Acoust. Soc. Amer.*, vol. 87, no. 3, pp. 1327–1335, Mar. 1990.

[25] J. F. Figueroa and J. Lamancusa, "A method for accurate detection of time-of-arrival—Analysis and design of an ultrasonic ranging system," *J. Acoust. Soc. Amer.*, vol. 91, no. 1, pp. 486–494, Jan. 1992.

[26] M. Toda and J. Dahl, "PVDF corrugated transducer for ultrasonic ranging sensor," *Sens. Actuators A, Phys.*, vol. 134, no. 2, pp. 427–435, Mar. 2007.

[27] M. Hazas and A. Ward, "A novel broadband ultrasonic location system," in *Proc. 4th Int. Conf. UbiComp*, Goteborg, Sweden, 2002, pp. 264–280.

[28] M. Parrilla, J. J. Anaya, and C. Fritsch, "Digital signal processing techniques for high accuracy ultrasonic range measurements," *IEEE Trans. Instrum. Meas.*, vol. 40, no. 4, pp. 759–764, Aug. 1991.

[29] G. S. Kino, *Acoustic Waves: Devices, Imaging, and Analog Signal Processing*. Englewood Cliffs, NJ: Prentice–Hall, 1987.

[30] H. Piontek, M. Seyffer, and J. Kaiser, "Improving the accuracy of ultrasound-based localisation systems," *Pers. Ubiquitous Comput.*, vol. 11, no. 6, pp. 439–449, Aug. 2007.

[31] J. Johansson, M. Gustafsson, and J. Delsing, "Ultra-low power transmit/receive ASIC for battery operated ultrasound measurement systems," *Sens. Actuators A, Phys.*, vol. 125, no. 2, pp. 317–328, Jan. 2006.

[32] R. Furutani and K. Kamahora, "Development of a new artifact for the calibration of large scale instruments," *Measurement*, vol. 30, no. 2, pp. 139–143, Sep. 2001.

[33] G. E. P. Box, W. G. Hunter, and J. S. Hunter, *Statistics for Experimenters*. New York: Wiley, 1978.
[34] V. Shnayder, M. Hempstead, B. Chen, M. Werner Allen, and M. Welsh, "Simulating the power consumption of large scale sensor network applications," in *Proc. SenSys*, Baltimore, MD, Nov. 3–5, 2004, pp. 188–200.

Fiorenzo Franceschini received the M.Sc. degree (*cum laude*) in nuclear engineering from the Politecnico di Torino, Torino, Italy, in 1984.

He is currently a Full Professor of quality management and the Head of the Department of Manufacturing Systems and Business Economics (DISPEA), Politecnico di Torino. Since August 1997, he has been a member of the European Experts Database as Evaluator of the research technological development proposals in industrial and materials technologies for the European community. He is author or coauthor of seven books and about 120 published papers in scientific journals and international conference proceedings. His current research interests are in the areas of quality engineering, statistical process control, QFD, and industrial metrology. He currently coordinates some important projects in the area of quality management for public and private organizations.

Mr. Franceschini is a Senior Member of the American Society for Quality and a Full Member of The Institute for Operations Research and Management Sciences (INFORMS).

Domenico Maisano received the M.Sc. degree (*cum laude*) in Mechanical Engineering in 2003 and the Ph.D. degree in "Systems for the Industrial Production" in 2008 from Politecnico di Torino, Italy.

From 2003 to 2005, he was involved in a project in the area of quality management with FIAT Auto. He is currently an Assistant Professor with Politecnico di Torino. He is the coauthor of two books and 20 publications on international journals and proceedings. His current research interests are industrial metrology and quality management. In particular, he is in charge of developing an indoor system to perform large-scale dimensional measurements.

Luca Mastrogiacomo received the M.Sc. degree (*cum laude*) in Mathematical Engineering in 2006 and the Ph.D. degree in "Systems for the Industrial Production" in 2009 from Politecnico di Torino, Italy.

He is currently with Politecnico di Torino. He is the coauthor of seven publications on international journals and proceedings. His research activities concern the study and testing of a wireless sensor network technology for distance measuring and position estimation. Other fields of interest are industrial metrology, quality management, and statistical process control.

Barbara Pralio received the M.Sc. degree in aerospace engineering in 2000 from Politecnico di Torino, Torino, Italy, where she is currently working toward the Ph.D. degree.

She was a Consultant and a Research Assistant for aircraft design and experimental flight dynamics research topics within national and international research programs with the Aerospace Engineering Department, Politecnico di Torino. She is currently a Research Assistant for study and development of innovative solutions for large-scale metrology applications with the Department of Production Systems and Business Economics, Politecnico di Torino. She has coauthored a number of technical papers in international journal and conferences in the areas of aircraft design, unmanned aerial vehicles applications, control systems, simulation, and target tracking.